



POSITRON TUNNELING MICROSCOPY

W. E. Frieze, D. W. Gidley and B. D. Wissman

Department of Physics, University of Michigan
Ann Arbor, MI 48109

(Received 19 March 1990 by E. Burstein)

A new technique for analyzing thin film growth processes, called positron tunneling microscopy (PTM), is proposed as an extension of the recently developed positron reemission microscope. The unique feature of a PTM is that image contrast is provided by the exponential reemission probability for positrons tunneling through thin-film overlayers that present an energy barrier to reemission. Results of positron tunneling experiments show that PTM should have monolayer thickness resolution to processes that locally affect either the tunneling barrier's width, such as islanding and subsurface roughness, or the barrier's energy, such as lattice strain in pseudomorphic growth and compositional mixing in interdiffusion alloying. In the case of these latter effects where there may be no topological contrasts at all, experimental results are discussed in greater detail. Comparisons of PTM with existing electron microscopies are presented where appropriate.

Characterization of the nucleation, growth, and defect structure of thin films is of critical importance in systematically and reproducibly studying multilayer systems. For films below 10Å thick there are relatively few techniques available that can provide suitable contrast and high lateral resolution for imaging analysis. Based on our studies of positron tunneling and reemission from thin multilayer systems [1,2] we conclude that a new technique, using the recently developed positron reemission microscope [3,4], should ultimately permit several Angstrom resolution imaging of morphological and/or chemical potential variations in a film that is only two or three atomic layers thick. We call this new technique positron tunneling microscopy (PTM). In this paper we discuss the basic positron tunneling process, how it would provide contrast in a PTM, and the lateral and thickness resolutions that can eventually be expected from improved positron microscopes. We will describe the basic physics of specific applications in thin film growth including the imaging of islands, pinhole defects, substrate roughness, lattice strain, and interdiffusion alloying. Where possible we will point out advantages and disadvantages of PTM relative to existing microscopies. However, we consider this new technique to be complementary to, rather than competitive with, electron techniques, since PTM may yield new information on systems for which electron images are presently not adequate.

A PTM is an ultra high vacuum positron reemission microscope (PRM) with a suitably chosen target for positron tunneling (to be discussed). A positron beam of high beam-optical brightness is generated us-

ing a positron source, a moderator, and two remoderators [5]. This beam of several keV kinetic energy is focused onto a target in which the positrons thermalize and, with some probability, diffuse back to the surface. If the positron work function of the surface is negative (as it is for many metals, see Reference 6 for a review) positrons can be reemitted with typical energies of order 1 eV. These positrons are accelerated and focused to form an image on a channel electron multiplier array (CEMA) coupled to a phosphor screen. Image contrast is provided by any mechanism that locally affects the transport to, or reemission from, the surface.

Positron transport in a multilayer system [1,7] is complicated by the fact that the positron ground state energy in each of the layers is different, and depends on the bulk chemical potential sum $\Sigma = \mu^+ + \mu^-$. Thus a positron implanted and thermalized in a substrate will encounter a potential energy change $\Delta\Sigma$ equal to the change in positron chemical potential $\Delta\mu^+$ plus an interface potential difference $\Delta\mu^-$ required by equilibrium of the electron Fermi levels across the interface. Measured values of Σ for some typical materials can be found in Reference 1. If the overlayer value of Σ is greater than that of the substrate, then positrons that have thermalized in the substrate must tunnel through the resultant energy barrier in order to be emitted from the surface. Such a sample, suitable for PTM analysis, is illustrated in Figure 1 for a Co film on Ni. In this case, $\Delta\Sigma$ is about 0.5 eV [1], assuming bulk Co growth on the Ni.

We have measured the tunneling "current" for positrons that have thermalized in Ni(100) and Ni(111) substrates as a function of the thickness of thin, epitaxially

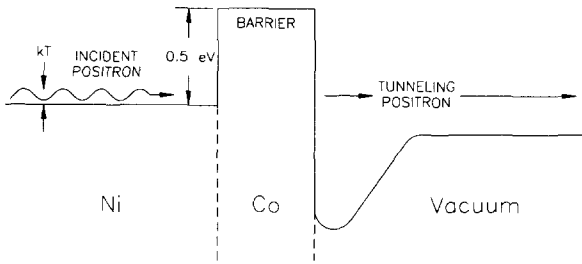


Figure 1. A simplified view of the tunneling of positrons (that have thermalized in a Ni substrate) through a Co overlayer. It is assumed that $\Delta\Sigma = 0.5$ eV corresponds to the difference in the bulk values of Σ .

grown, Co overlayers (see Figure 2). The rate of re-emission is observed to decrease roughly exponentially for increasing overlayer thickness h , with an exponential constant of 1.5–2.0 Å. If we ignore the detailed shape of the barrier and assume it to be square, then the tunneling probability P should asymptotically approach

$$P \propto e^{-\frac{h}{\alpha}} \quad \text{with} \quad \alpha^{-1} = \frac{\sqrt{8m(\Delta\Sigma - E)}}{\hbar}$$

where E , the positron kinetic energy in the substrate, is typically thermal. For the Co on Ni sample, we thus expect α to be about 1.4 Å, in reasonable agreement

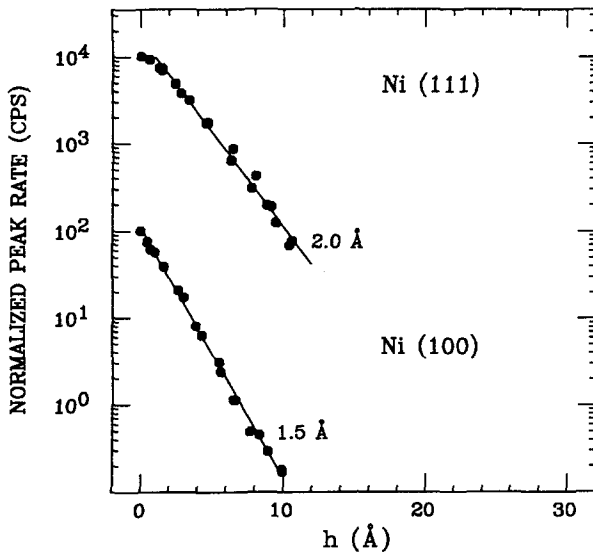


Figure 2. Experimental results for positrons tunneling through epitaxially grown overlayers of Co on single crystal Ni substrates. The overlayer thickness h is determined by Auger spectroscopy and has a systematic uncertainty of about 20%. The ordinate is the count rate of reemitted positrons in the Ni energy peak, normalized to 10^4 and 10^2 respectively at $h = 0$. The technique of reemitted positron energy spectroscopy is discussed in Reference 1.

with our observations. It is this exponential dependence of the positron tunneling probability on film thickness and barrier height $\Delta\Sigma$ that can produce sharp contrast in a PTM for small changes in morphology that affect these parameters. As a result, the most straightforward use of the PTM is to image film thickness variations at different stages of nucleation and growth. As depicted in Figure 3, islanding, steps and ledges, and pinhole defects in the overlayer could be imaged with monolayer thickness resolution. In addition, subsurface roughness due to interfacial instability during the growth process could be imaged under some circumstances even if the overlayer surface is perfectly flat. Thus the PTM could be used to systematically monitor the growth mode and quality of a thin film overlayer with monolayer thickness resolution under most circumstances. Before turning to other applications in film growth we will first consider the lateral resolution to be expected for a PTM.

Given certain estimates for the size of the radioactive source, and the operation of the moderators and remoderators, we can estimate the brightness of the positron beam in a PRM. This is the primary factor that determines the lateral resolution of the image. In particular, we use values that we ultimately hope to achieve in our own positron microscope construction project over the next several years. Taking a source activity of order 100 Ci of ^{58}Co (15% β^+ emission branching ratio), and

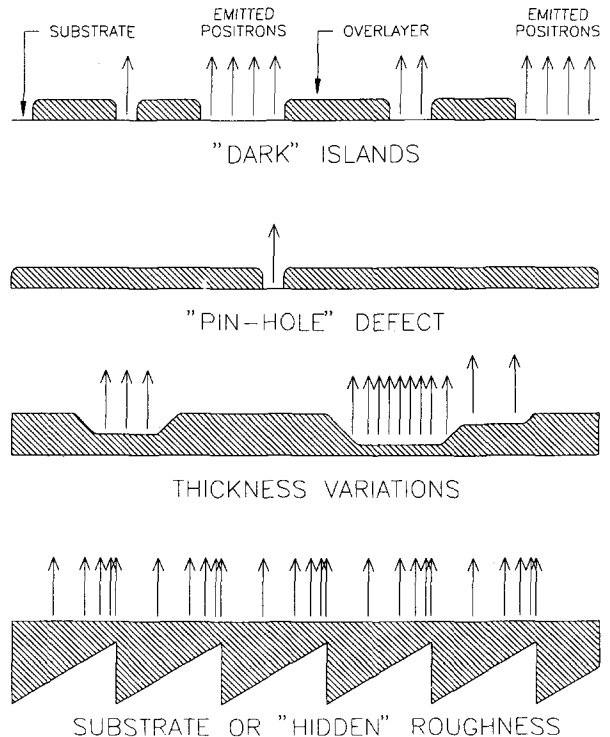


Figure 3. Simplified representation of several types of thickness variations in thin film overlayers that could be observed in a PTM.

an initial moderator efficiency of 1×10^{-3} , we obtain an initial (un-remoderated) positron beam rate of roughly 6×10^8 e^+ /s. For two remoderators of 10% efficiency each, this yields 6×10^6 e^+ /s on target. Brightness enhancement calculations applied to the emittance of a typical positron moderator (assuming a 5 mm diameter radioactive source) yield a final beam diameter on target of around $5 \mu\text{m}$ at a final beam energy of 4 keV. Using typical spherical aberration coefficients for the objective lens of an emission-microscope optical system [8], we can estimate the overall resolution for any given exposure time and any desired, counting-statistics limited, signal-to-noise ratio. Taking an exposure time of one hour and a 30:1 signal-to-noise ratio, we obtain [9] an expected resolution of approximately 15 Å. Ultimately, we expect this figure to approach several Angstroms as remoderators are perfected (and perhaps cooled) and as more intense positron sources are utilized.

By way of comparison, many of the overlayer topological features visible with PTM might also be studied by scanning electron microscopy (SEM). This technique is very sensitive to surface topology, and like PTM, can be used directly with thick samples. SEM is however, primarily a surface technique, being relatively insensitive to most subsurface features. In addition, its resolution tends to be in the 50–100 Å regime for most instruments, with higher resolutions generally involving increased incident beam energy, which can lower contrast or damage samples. Thus, while many of the surface topological features visible to PTM might also be observable using SEM, most interface topology would not. Moreover, the expected ultimate resolution of a PTM should be several times better than that usually available using SEM, although PTM exposure times will generally be much longer. This emphasizes the complementary nature of PTM and electron microscopies: a scanning electron microscope incorporated into a positron microscope would serve as an excellent probe for locating target features for more detailed study with higher resolution PTM.

Since the tunneling probability of a positron through an overlayer depends exponentially on both h and $\Delta\Sigma$, a PTM micrograph is, in effect, an image of overlayer thickness for constant Σ (as depicted in Figure 3), or an image of the local value of Σ for constant thickness. This latter effect of direct sensitivity to chemical potential appears to be a unique attribute of PTM. It opens a wide range of physical phenomena in overlayer systems to study using a PTM, since many phenomena can affect the value of Σ in the overlayer. One example is strain in the overlayer lattice, or in other words a change in overlayer lattice constant from its bulk value. Because of the large positron deformation potential of many materials [10], typically $-(10-15)\text{eV}$, a strain-induced volume expansion of several percent can change Σ of an overlayer, and hence $\Delta\Sigma$, by nearly 0.5 eV. Thus PTM can be very sensitive to small changes in overlayer lattice constant.

An example [2] of this is given in Figure 4. There we plot data on the number of positrons reemitted through thin overlayers of Ni grown epitaxially on Cu(110) and Cu(111) substrates, as a function of the overlayer thickness. This system exhibits pseudomorphic growth of the Ni until a critical thickness is reached ($h_c \approx 14$ Å). At this point, misfit dislocations appear and the overlayer lattice constant relaxes to essentially the bulk value. During the pseudomorphic phase, Σ of the overlayer is strain-shifted downward from its bulk value by just over 0.5 eV. This is larger than the 0.5 eV value of $\Delta\Sigma$ between unstrained Ni and Cu, and thus during pseudomorphic growth the tunneling barrier *disappears*. The slope of the data in the pseudomorphic region for the semi-logarithmic plot of Figure 4 (~ 22 Å) is consistent with the mean free path of a low energy positron traveling through the overlayer [11]. Only beyond the critical thickness does the slope revert to a value that is more consistent with tunneling through a barrier (see Reference 2 for a more detailed discussion).

Thus a PTM should be able to image strain in an overlayer as thin as 1–2 monolayers. Depending on the particular values of $\Delta\Sigma$ and the deformation potential, strain-induced variations in lattice constant of 1% or less should be readily visible in such images. PTM strain images acquired in-situ at various stages of film growth as average film thickness goes through h_c should provide a very interesting local view of the pseudomorphic

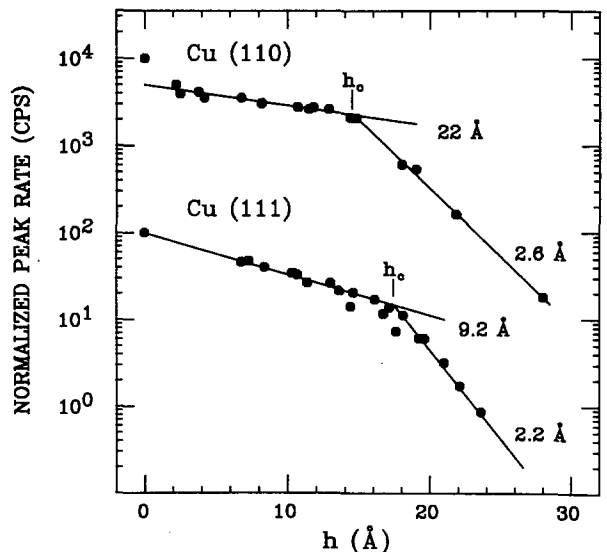


Figure 4. Reemitted positron energy spectroscopy results (reproduced from Reference 2) for epitaxial Ni films of thickness h grown on Cu substrates (and annealed at 200°C). The ordinate is the count rate of reemitted positrons in the Cu energy peak, normalized to 10^4 and 10^2 at $h = 0$ as in Figure 2. The critical thickness h_c for pseudomorphic growth is indicated by a sudden change in the exponential slope.

growth transition and subsequent lattice relaxation. Images of lattice strain near steps and ledges may yield significant information on overlayer growth mechanisms. Strained regions such as those surrounding a dislocation may act to trap charge or impurities, thereby changing the chemical activity of these sites in catalytic systems. Thus in chemical catalysis research, as well as materials research, a PTM micrograph showing the location of strain in an overlayer should be extremely useful.

The traditional electron microscopy for studying strain in an overlayer is transmission electron microscopy (TEM). Strain is observed through its diffractive effects on the electron beam [12]. The primary advantages of TEM are high resolution and an ability to observe subsurface features. Its disadvantages are a need for very thin samples, and low contrast in cases where the substrate and overlayer have similar electron scattering cross sections. It is unlikely that PTM will be able to obtain resolutions comparable to the best TEM resolutions because of the relatively large aberrations in the objective lens used to accelerate the reemitted positrons away from the target, and because of the low intensity of positron beams relative to electron beams. (The former problem is inherent in all reemission microscopies. [13]) However, image contrast for such effects as overlayer strain should be much higher for the PTM, because of the exponential dependence of the tunneling probability on $\Delta\Sigma$. Furthermore, there is no need for thin samples. Thick, robust targets can be used directly without prior preparation, and can be studied during in-situ operations such as film coating, sputtering, heating, or chemical catalysis. This property is common to most positron microscopies [3], and represents a significant advantage. In addition, PTM analysis is not damaging to most samples, as both current density and absorbed radiation dose are quite small [4]. Thus, in general, positron microscopy should be considered a non-destructive testing method.

Another overlayer property that can influence Σ and hence $\Delta\Sigma$, is chemical composition [1]. In Figure 5 we show the variation in Σ for Ni-Cu substitutional alloys as a function of composition. As can be seen from the figure, the chemical potential sum varies more or less linearly with fractional composition from its pure Cu value to its pure Ni value. Because of the exponential dependence of the tunneling probability on $\Delta\Sigma$, a PTM image should thus be a very sensitive measure of the chemical or alloy composition of an overlayer. A PTM micrograph might then be regarded as an image of impurity distribution, provided the local concentration is high enough to shift $\Delta\Sigma$ by a measurable amount. A high-resolution image of the distribution of impurities in an overlayer can be very useful in a variety of systems. Studies of interdiffusion alloying, impurity migration and aggregation, grain boundary diffusion, and spiking of the substrate through the overlayer should all be possible using the PTM technique.

The electron microscopy that is most directly sensitive to chemical composition is scanning Auger microscopy (SAM). This technique is similar to SEM, the difference being that the signal detected is Auger electron emission rather than secondary electron emission. Thus SAM is primarily sensitive to chemical composition up to a depth of about 10 Å below the sample surface, a depth roughly comparable to that accessible to PTM. Because of the low probability of Auger emission as opposed to secondary electron emission, the resolution of a typical SAM is generally at least an order of magnitude worse than that of a typical SEM. Thus PTM resolutions should be significantly better than those of SAM. This is particularly important since many of the structures (islands, steps, etc.) that are of interest in studies of micro-chemical-composition are below the resolution limit of the SAM technique.

Finally, we should point out the strong connection between PTM and scanning tunneling microscopy (STM). STM offers resolution better than any other microscopy, and it is rapidly finding more and more applications. The PTM and STM methods both depend on tunneling currents, STM on the tunneling of electrons through a surface potential barrier to a nearby probe tip, and PTM on the intrinsic tunneling behavior of positrons through the potential barrier presented by a thin overlayer. Thus it should be extremely interesting to compare STM and PTM micrographs of the same sample. One of the contrasts between the two techniques is

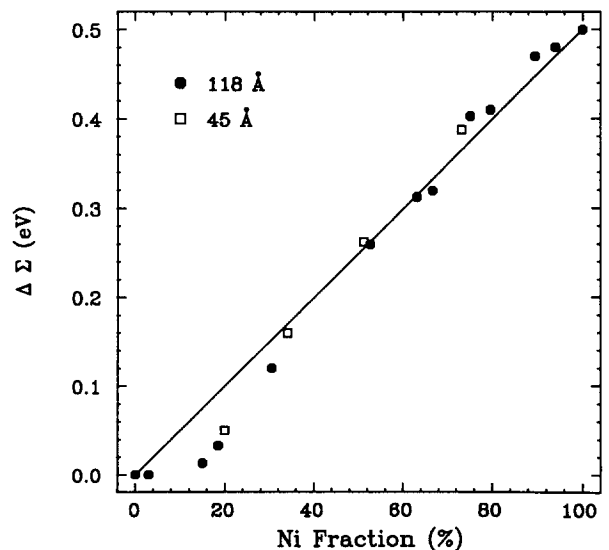


Figure 5. The shift in the overlayer value of Σ from that of pure Cu plotted as a function of Ni alloy fraction (as determined by Auger spectroscopy) for films that were deposited as pure Cu on a Ni(110) substrate. The sample was heated for 2 minutes at successively higher temperatures up to a maximum of 930°C to induce interdiffusion alloying. These data are replotted from Reference 1.

the fact that PTM is directly sensitive to the overlayer thickness while STM is sensitive to the overall topology of the surface. Thus interfacial topology as opposed to surface topology should be more readily visible using PTM. Another difference is the fact that a sample contains many electrons, but generally (even in a high flux beam) at most a single positron. Thus differences in electron energy levels from point to point in a material are masked by the internal electric fields generated by charge migrating to regions of reduced potential energy. That is, the Fermi level of a metal is forced by the flow of charge to be spatially constant just as it must be between substrate and overlayer. Positron energy levels on the other hand, can change as one moves from one point in a sample to another, for example, from a region

of low to one of high strain. Thus, although there are many similarities between PTM and STM, there are also many differences, and it will be particularly interesting comparing the two methods when PTM resolution approaches the tens of Angstroms level.

Acknowledgement – We thank our colleagues Arthur Rich and James Van House for many discussions concerning positron microscopy. We also thank Johannes Schwank, Fred Terry, and Ken Wise for helpful discussions of PTM applications. This work is supported by National Science Foundation grant DMR-8618721, Department of Energy grant DE-FG02-90ER12103, and the Office of the Vice-President for Research of the University of Michigan.

REFERENCES

1. D. W. Gidley and W. E. Frieze, *Phys. Rev. Lett.* **60**, 1193 (1988).
2. D. W. Gidley, *Phys. Rev. Lett.* **62**, 811 (1989).
3. James Van House and Arthur Rich, *Phys. Rev. Lett.* **61**, 488 (1988).
4. G. R. Brandes, K. F. Canter, and A. P. Mills, Jr., *Phys. Rev. Lett.* **61**, 492 (1988).
5. See for example, W. E. Frieze, D. W. Gidley, and K. G. Lynn, *Phys. Rev. B* **31**, 5628 (1985), and the references therein.
6. Peter J. Schultz and K. G. Lynn, *Rev. Mod. Phys.* **60**, 701 (1988).
7. P. A. Huttunen, J. Mäkinen, and A. Vehanen, to be published in *Phys. Rev. B*.
8. A. B. El Kareh and J. C. J. El Kareh, *Electron Beams, Lenses, and Optics*, Volume 2 (Academic Press, New York, 1970).
9. Detailed PRM resolution calculations will be published elsewhere. See also estimates of resolution in References 3 and 4.
10. See Reference 2 and the references therein.
11. R. M. Nieminen and J. Oliva, *Phys. Rev. B* **22**, 2266 (1980); and P. A. Huttunen, A. Vehanen, and R. M. Nieminen, to be published in *Phys. Rev. B*.
12. See for example, G. Honyo and K. Yagi in *Current Topics in Material Science*, Volume 6, edited by E. Kaldis (North-Holland, Amsterdam, 1980).
13. See for example, G. H. Griffith, *Appl. Surf. Sci.* **26**, 265 (1986), and the references therein.